Supporting Information

Enhanced photoelectric conversion efficiency of dye-sensitized solar cells by the incorporation of dual-mode luminescent $NaYF_4:Yb^{3+}/Er^{3+}$

Ying Li, Kai Pan, Guofeng Wang*, Baojiang Jiang, Chungui Tian, Wei Zhou, Yang Qu, Shuai Liu, Li Feng, and Honggang Fu*

Key Laboratory of Functional Inorganic Material Chemistry, Ministry of Education, School of Chemistry and Materials Science, Heilongjiang University, Harbin, 150080, P. R. China. E-mail: wanggf75@gmail.com; fuhg@vip.sina.com

Table S1. Solar cell parameters of TiO_2-$NaYF_4$ cell under simulated solar light with a UV cutoff filter ($\lambda \geq 400$ nm).

DSSC	I_{sc}(mA/cm^2)	V_{oc}(V)	FF	η(%)
TiO_2-$NaYF_4$	5.5275	0.698	0.71	2.80

Figure S1. XRD patterns of $NaYF_4:Yb^{3+}/Er^{3+}$ microcrystals after sintering at 450 °C for (a) 2h and (b) 4h in an argon atmosphere.

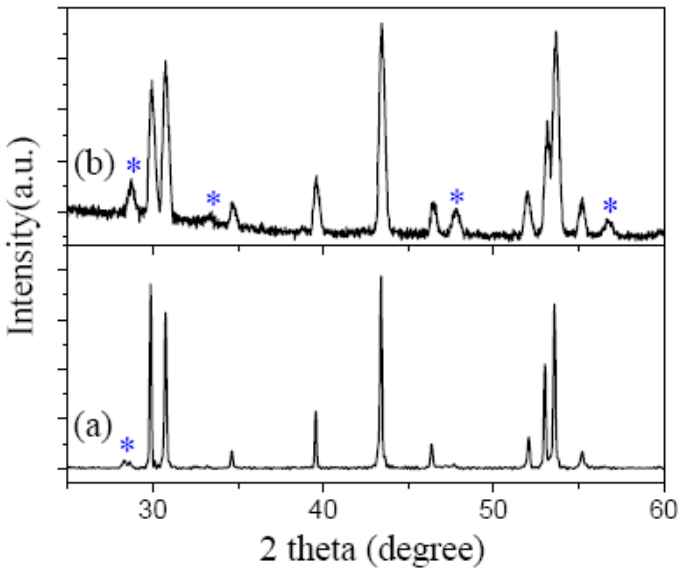

5

Figure S2. SEM images of $NaYF_4:Yb^{3+}/Er^{3+}$ microcrystals after sintering at 450 °C for (a,b) 2h and (c,d) 4h in an argon atmosphere.

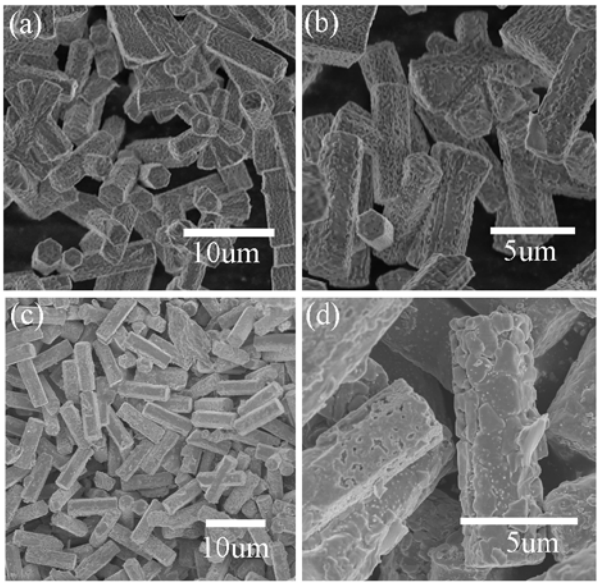

Figure S3. The absorption spectrum of the N719 dye.

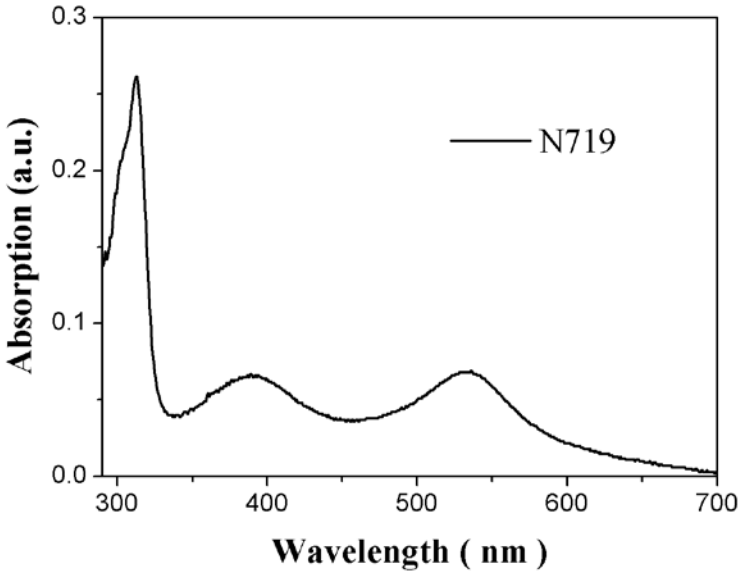

Figure S4. The UV-Vis absorption spectra of desorption dye from N719-sensitized TiO_2 and TiO_2-$NaYF_4$:Yb^{3+}/Er^{3+} photoanodes

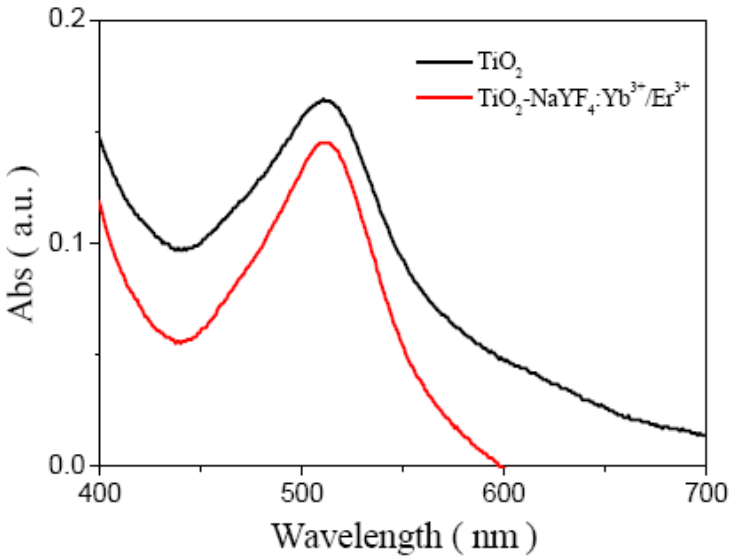

Figure S5. Comparison of diffusion lengths of TiO_2 and TiO_2-$NaYF_4$:Yb^{3+}/Er^{3+} photoanodes.

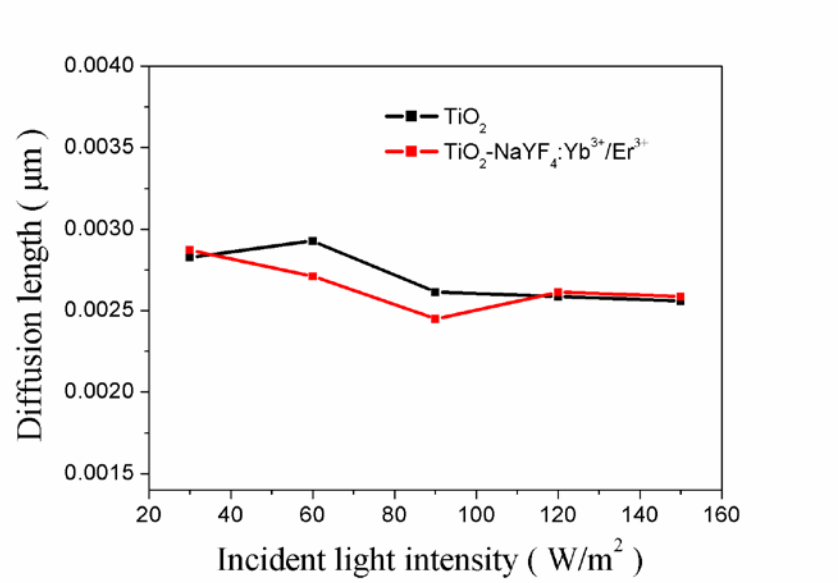

Figure S6. Comparison of diffusion coefficients of TiO_2 and TiO_2-$NaYF_4$:Yb^{3+}/Er^{3+} photoanodes.

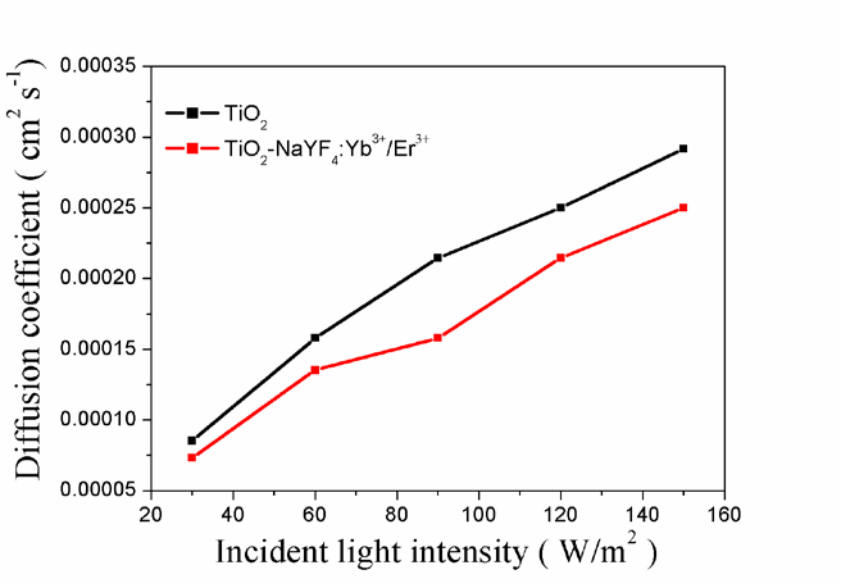

Figure S7. Comparison of diffuse reflectance spectra of TiO_2 and TiO_2-$NaYF_4$:Yb^{3+}/Er^{3+} photoanodes.